Excited-State Behavior and Photoionization of 1,8-Acridinedione Dyes in Micelles—Comparison with NADH Oxidation

Chellappan Selvaraju[a] and Perumal Ramamurthy*[a, b]

Abstract: The photophysics and photochemistry of 1,8-acridinedione dyes, which are analogues of reduced nicotinamide adenine dinucleotide (NADH), are studied in anionic and cationic micelles. Acridinedione dyes (ADDs) are solubilized in micelles at the micelle–water interface and are in equilibrium between the aqueous and micellar phase. The binding of the ADDs with micelles is attributed to hydrophobic interactions and the binding constants are determined with steady-state and time-resolved techniques. Nanosecond laser flash photolysis studies are carried out in aqueous, anionic, and cationic micellar solutions. The ADD undergoes photoionization in the excited state to give a solvated electron. The solvated electron reacts with the ADD to give an anion radical. In anionic micelles, the yield of the solvated electron increases because of the efficient separation of the cation radical and the electron. Cation radicals derived from the photooxidation of ADDs are involved in keto–enol tautomerization. Under acidic conditions, an enol radical cation of the acridinedione dye is formed from the keto form of the cation radical by intramolecular hydrogen atom transfer. In cationic micelles, due to electrostatic attraction, the electron cannot escape from the micelle and recombination of the cation radical and the electron results in the formation of a triplet state. For the first time, a solvated electron is observed in the laser flash photolysis of ADDs in anionic micelles. The photoionization of ADDs depends on the excitation wavelength and is biphotonic at 355 nm and monophotonic at 248 nm. From the results with this NADH model compound, the sequential electron–proton–electron transfer oxidation of NADH is confirmed and the nature of the intermediates involved in the oxidation is unraveled; these intermediates are found to depend on the pH value of the medium.

Keywords: acridinedione · cofactor models · micelles · photooxidation · radical ions

Introduction

Reduced nicotinamide adenine dinucleotide (NADH) plays a vital role as the electron source in the reduction of oxygen in the respiratory chain.[1] The biological activity of oxidized nicotinamide adenine dinucleotide (NAD^+) and NADH is based on the ability of the nicotinamide group to undergo a reversible oxidation–reduction reaction. The mechanisms of the conversion of NADH into NAD^+ and of the reverse reaction have been studied extensively in coenzymes as well as in synthetic analogues during the last two decades.[2] The issue of whether the conversion involves a one-step hydride transfer[3] or a stepwise electron–proton–electron transfer[4] has been studied extensively. An NADH radical cation formed as an intermediate in the photooxidation of NADH is confirmation of the sequential electron–proton–electron transfer mechanism. Evidence to support the operation of such a mechanism during thermal, photochemical, and electrochemical oxidation of NADH and its analogues has been reported.[5] Photoinduced electron transfer reactions of NADH model compounds with various one-electron oxidants have been reported.[6]

Acridinedione dyes (ADDs; for example, **1** and **2**) have been developed recently as a family of efficient laser dyes[7]

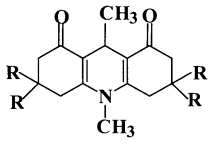

ADD **1** R=H

ADD **2** R=CH_3

[a] Dr. C. Selvaraju, Dr. P. Ramamurthy
Department of Inorganic Chemistry
University of Madras, Guindy Campus
Chennai 600 025 (India)
Fax: (+91) 044-22300488
E-mail: prm60@hotmail.com

[b] Dr. P. Ramamurthy
National Centre for Ultrafast Processes
University of Madras, Taramani Campus
Chennai 600 113 (India)
E-mail: prm60@hotmail.com

 DOI: 10.1002/chem.200305678

and these dyes have structural similarity with NADH. These dyes have been shown to mimic NADH analogues to a great extent because of their tricyclic structure, which is capable of protecting the enamine moiety.[8] Drugs such as nifedipine, nimoldipine, and nisoldipine fall into this class and have many applications in medicine, for example, as calcium antagonists, antihypertensive agents, and antiinflammatory drugs.[9] These dyes can function as both electron donors and acceptors and their electrochemical,[10] photophysical,[11] and excited-state reactions[12] in homogeneous solution have been investigated.

Photoionization also plays an important role in biological processes; a good example is light interaction in chloroplasts during photosynthesis.[13] The photoionization of NADH derivatives has been investigated with respect to the biological process.[14] Both monophotonic and biphotonic photoionization of NADH has been reported.[15]

A micelle can serve as a structural and functional model for complex bioaggregates, including proteins and biomembranes.[16] The unique and different photophysical properties observed in micelles are due to a number of factors, such as solute distribution, mobility, conformational restraints, and the local electrical field. Within a distance of a few nanometers, the microscopic dielectric constant varies from 2 to 80 Debye units and the microviscocity changes by an order of magnitude. These factors give rise to some fascinating dimensions for photoinduced processes, both chemical and physical, that occur in the micelle.[17] Micelles are recognized as a good means of compartmentalizing solutes and they increase the ion yield by preventing the back electron transfer of the ion pair. In particular, the micellar system strongly promotes the photoionization of many aromatic molecules.[18,19] We report here the photophysics and photochemistry of the acridinedione dyes in aqueous medium and in anionic and cationic micelles; this study includes photoionization of the dyes. We also report the role of the pH value in the mechanistic pathway of oxidation of the acridinedione dyes, a role that can be extended to NADH oxidation.

Results and Discussion

Absorption and fluorescence: The absorption spectra of ADD **1** were measured in water and with various concentrations of surfactant. The critical micellar concentrations (CMCs) of sodium dodecylsulfate (SDS) and cetyltrimethylammonium bromide (CTAB) micelles are 8.2 and 0.92 mM, respectively.[20] Below the CMC, there is no change in the intensity of the absorption peak of ADD **1** at 390 nm with either SDS or CTAB. Above the CMC, the absorbance decreases as the concentration of the surfactant increases, with a simultaneous shift in the absorption maximum towards the blue region; these changes are most rapid at the CMC. The long-wavelength absorption maximum depends on the solvent polarity and is assigned to intramolecular charge transfer.[11] The absorption maxima of ADD **1** in micelles and in various homogeneous solvents with different polarities are listed in Table 1. With decreasing solvent polarity the absorption maximum is blue shifted and there is a decrease in the molar extinction coefficient. The blue shift of the absorption maximum and the decrease in the molar extinction coefficient observed in the micelles are similar to this solvent effect. This indicates that the ADDs are transferred from the bulk aqueous to the less polar micellar environment.

Table 1. Absorption and fluorescence maxima and fluorescence quantum yield of ADD **1** in various solvents.

Solvent	Absorption λ_{max} [nm] (ε [$M^{-1}cm^{-1}$])	Fluorescence λ_{max} [nm]	ϕ_f	$E_T(30)$
water	396 (9823)	470	0.45	63.1
methanol	378 (9332)	456	0.91	55.4
acetonitrile	370 (8912)	444	0.90	45.6
acetone	370 (8128)	441	0.88	42.2
dichloromethane	370 (7762)	440	0.90	40.7
chloroform	372	438	0.92	39.1
ethyl acetate	370	437	0.89	38.1
SDS	392 (9009)	462	0.74	–
CTAB	390 (9152)	463	0.71	–

The effect of surfactant concentration on the emission spectrum of the ADD **1** is shown in Figure 1. Below the CMC, there is no change in the emission intensity and emission maximum of the dye on excitation at a isosbestic point (378 nm). As the concentration of surfactant increases above the CMC, the fluorescence intensity is enhanced and there is a blue shift in the emission maximum. The fluorescence maxima and emission quantum yields of ADD **1** in micelles and in various homogeneous solvents with different polarities are listed in Table 1. The polarity-dependent emission maximum confirms the charge-transfer character of the S_1 state. The fluorescence enhancement of several dyes in

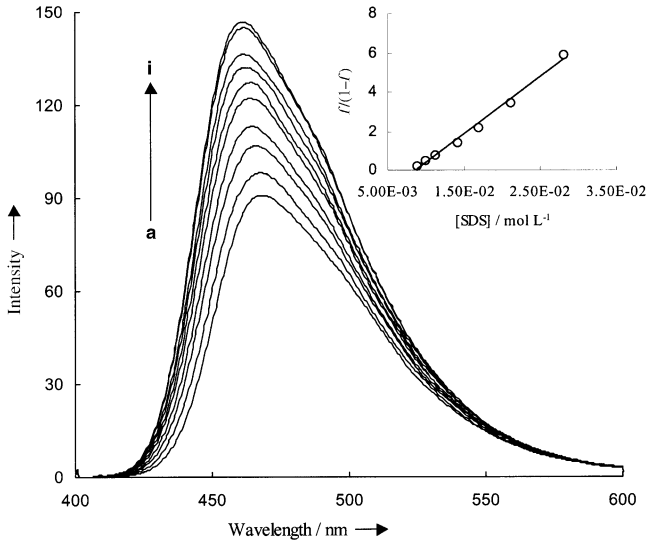

Figure 1. Emission spectrum of ADD **1** in water with SDS concentrations of a) 0, b) 8.4×10^{-3}, c) 9.8×10^{-3}, d) 0.011, e) 0.014, f) 0.017, g) 0.021, h) 0.0634, and i) 0.11 M. Inset: Plot of $f/(1-f)$ against concentration of SDS for ADD **1**.

micelles has been reported.[21–23] Chouchiang and Lukton[22] reported the fluorescence enhancement of 2-(*p*-toluidinyl)-naphthalene-6-sulfonate (TNS) in SDS micelles, an enhancement due to the interaction between the micelles and the TNS. The fluorescence enhancement of cyanine and rhodamine dyes in micelles has also been reported.[23] These dyes undergo aggregation in aqueous solution and, due to this, they have lower fluorescence quantum yields in homogeneous solvents. The fluorescence enhancement of these cyanine and rhodamine dyes in micelles is due to the prevention of aggregation of the dyes. The aggregation of ADDs in homogeneous solvents is not possible because these dyes are nonplanar; with increasing concentration of the ADD, we do not observe any new peak in the absorption and emission spectra. The fluorescence enhancement of ADD molecules by micelles is not due to the prevention of aggregation processes observed with the cyanine and rhodamine dyes.

Bagdasarian and Shahinyan[24] reported the association of dye molecules on the micellar surface and this affects the absorption and fluorescence characteristics of the dyes. The fluorescence enhancement of ADDs in micelles was analyzed by the Benesi–Hildebrand equation [Eq. (1)],[25] where K is the equilibrium constant, $[M]$ is the concentration of micelles, and I_0, I', and I are the fluorescence intensity of ADD in the absence of micelles, the fluorescence intensity of bound ADD, and the measured fluorescence intensity, respectively.

$$\frac{1}{I_0-I}=\frac{1}{I_0-I'}+\frac{1}{K(I_0-I')[M]} \qquad (1)$$

The dependence of $1/I_0-I$ on the reciprocal concentration of micelles was found to be linear, a fact that indicates 1:1 binding. This confirms the absence of dimer formation on the surface of the micelle. Moreover, the absence of a new peak in the absorption and emission spectra excludes dimer formation of the acridinedione dyes.

The increase in the fluorescence intensity of intramolecular-charge-transfer emissions of ADD **1** and the corresponding blue shift of the emission maximum in micelles with respect to the results obtained with pure water are accounted for by the following reasons.

1) During the formation of micellar aggregates the ADD molecules are transferred from the highly polar aqueous phase to the less polar micellar environment. It is known that the excited singlet state of ADDs is more polar than the singlet ground state, a fact that is obvious from the dipole-moment data of these dyes. Experimentally observed dipole moments of the ground and excited states of ADDs are approximately 1.9 and 3.2 D, respectively.[11] Therefore, the S_1 state becomes less stabilized than the corresponding ground state in the less polar Stern layer of the micelles. As a result, the energy gap between the S_1 and S_0 states increases and there is consequently a shift in the emission maximum towards the blue region. The fluorescence spectral shift can be used to determine the polarity of the ADD binding site in micelles. A calibration curve was constructed by plotting the emission wavenumber against the polarity parameter, the $E_T(30)$ value. This allowed us to estimate the $E_T(30)$ values of the ADD binding sites as 57.5 and 59 for SDS and CTAB, respectively. On comparing these values with those of alkanes, like hexane (31), and water (63), it can be determined that the ADD is located neither in the core nor in the aqueous phase but is located at the micelle–water interface.
2) The fluorescence intensity enhancement in micelles is due to inhibition of radiationless decay by the micellar aggregates. This may be reasoned out in terms of rigidization of the ADDs in the local environment encountered in the micelle.[22]
3) In aqueous solution, the strong hydrogen-bonding interactions of water molecules with the dye induces nonradiative relaxation and therefore a decrease in the fluorescence quantum yield is observed.[26]. In micelles, ADD molecules are transferred from the hydrophilic aqueous phase to a hydrophobic micellar environment, which minimizes the hydrogen-bonding interactions between the ADD and water. This minimization of hydrogen-bonding interactions causes the diminution of radiationless relaxations (induced by hydrogen-bonding interactions) of the ADD, with a resultant enhancement of intramolecular-charge-transfer emission intensity in the micellar environment.

Fluorescence lifetimes: Fluorescence lifetimes of the ADDs were recorded in water and in different concentrations of SDS and CTAB solution. Below the CMC, all the dyes exhibit single exponential fluorescence decay with a lifetime of around 4–4.5 ns in water. Above the CMC, the fluorescence decay of the dyes does not obey a single exponential fit but instead follows a biexponential fit according to Equation (2), where $I(t)$ is intensity at time t, A_1 and A_2 are the preexponential factors, and τ_1 and τ_2 are fluorescence lifetimes. The emission decay profile of ADD **1** monitored at 470 nm and with different SDS concentrations is shown in Figure 2.

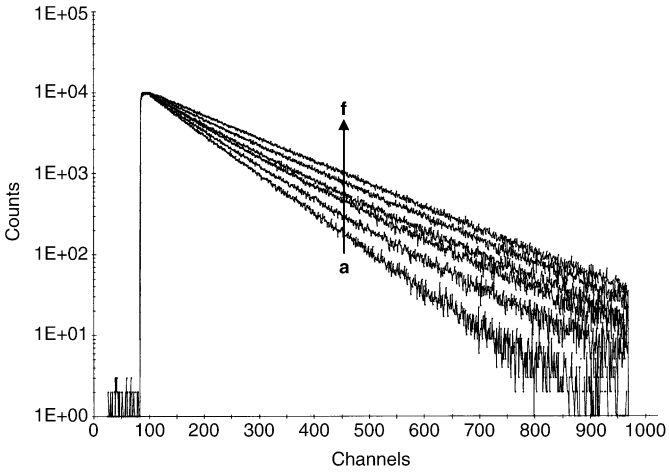

Figure 2. Fluorescence decay of ADD **1** in water with SDS concentrations of a) 0, b) 8.4×10^{-3}, c) 9.8×10^{-3}, d) 0.011, e) 0.014, and f) 0.11 M.

$$I(t) = A_1\exp\left(\frac{-t}{\tau_1}\right) + A_2\exp\left(\frac{-t}{\tau_2}\right) \quad (2)$$

In aqueous micellar solution, three possible locations, namely, the hydrophobic core, the bulk water, and the Stern layer, are available for the dyes. The biexponential behavior in the presence of micelles suggests that the ADDs are present in two different environments, in one of which the fluorescence decay of the ADDs has a shorter lifetime (4.2 ns) while in the other it has a longer lifetime (7.8 ns). The shorter lifetime is the same as the fluorescence lifetime of ADDs in water. The longer lifetime is assigned to the ADD molecules bound to the micelles. The biexponential analyses of ADDs in the presence of different concentrations of surfactant were carried out by fixing τ_1 as the lifetime of the dyes in water. The fluorescence lifetime data of ADD **1** are compiled in Table 2. With increasing surfactant concentration, the relative amplitude of fluorescence from the aqueous portion (B_1) decreases whereas the relative amplitude of fluorescence from the micelle portion (B_2) increases (Table 2). This confirms that the ADD is in equilibrium between these two environments.

Binding constants: The binding constants of ADD molecules with anionic and cationic micelles (SDS and CTAB) were determined by using both steady-state and time-resolved fluorescence techniques.

Steady-state fluorescence technique:[27] In the steady-state fluorescence technique, change in the fluorescence intensity of the ADD with surfactant concentration was used to determine the binding constants. Consider the equilibrium shown in Equation (3). The equilibrium constant for this reaction, K_s, is given by Equation (4), where $[D_a]$ and $[D_m]$ are the substrate (dye) concentrations in the aqueous phase and in the micellar phase, respectively. $[S_m]$ is the molar concentration of surfactant in the form of micelles and is equal to the total surfactant concentration minus CMC in the absence of dye.

$$D_a + S_m \rightleftharpoons D_m \quad (3)$$

$$K_S = \frac{[D_m]}{[D_a][S_m]} \quad (4)$$

The total dye and surfactant concentrations, $[D_t]$ and $[S_t]$, are given by Equations (5) and (6). In the presence of ADD dye the total surfactant concentration in the form of the micelle is the sum of the surfactant concentration in the form of the micelles with ADD [Dm] and without ADD [Sm].

$$[D_t] = [D_a] + [D_m] \quad (5)$$

$$[S_t] = [S_m] + [D_m] + CMC \quad (6)$$

The fraction of the dye associated with the micelle, f [Eq. (7)], can be expressed by Equation (8), where I, I_a, and I_m are the fluorescence intensities at an intermediate concentration of surfactant, in aqueous solution, and when the ADD is completely solubilized (that is, at 0.1 M surfactant concentration), respectively.

$$f = \frac{[D_m]}{[D_t]} \quad (7)$$

$$f = \frac{I - I_a}{I_m - I_a} \quad (8)$$

By combining Equations (4)–(8), we get Equation (9).

$$\frac{f}{1-f} = K_s([S_t] - [D_t]f) - K_s CMC \quad (9)$$

By making the approximations that $[D_m] \ll [S_t]$ and $[S_t] \gg$ CMC, Equation (9) can be reduced to Equation (10), where K is the binding constant and N is the aggregation number. The plot of $f/1-f$ against [S] gives a straight line, (Figure 1, inset) and the binding constant is calculated from the slope.

$$\frac{f}{1-f} = K_s[S_t] \quad (10)$$

$$\text{Slope} = \frac{K}{N}$$

Time-resolved fluorescence technique: In presence of micelles, the fluorescence decay of ADDs is biexponential with lifetimes of τ_1 and τ_2 and amplitudes of A_1 and A_2. The binding constant is calculated from the amplitude by using Equation (11), where [M] is the concentration of micelles as given by Equation (12).

$$\frac{A_2}{A_1} = K[M] \quad (11)$$

$$[M] = \frac{[S_t] - CMC}{N} \quad (12)$$

The binding constant is obtained from the slope of the plot of A_2/A_1 against [M]. The binding constants obtained from the time-resolved fluorescence technique are in close agreement with the values ob-

Table 2. Lifetime data for ADD **1**.

[SDS] [M]	Lifetime [ns]		Preexponential factor		Relative amplitude	
	τ_1	τ_2	A_1	A_2	B_1	B_2
0.00	4.42	–	–	–	100	–
8.44×10^{-3}	4.42	7.82	0.729	0.139	74.78	25.22
9.85×10^{-3}	4.42	7.81	0.569	0.295	52.16	47.84
0.0113	4.42	7.84	0.458	0.394	39.65	60.55
0.0141	4.42	7.80	0.344	0.512	27.52	72.48
0.0169	4.42	7.82	0.238	0.612	18.02	81.98
0.0211	4.42	7.85	0.163	0.674	12.03	87.97
0.0282	4.42	7.79	0.122	0.719	8.75	91.25
0.0634	4.42	7.82	0.050	0.806	3.39	96.61

tained by using steady-state fluorescence measurements and are compiled in Table 3.

Electrostatic and hydrophobic interactions are responsible for binding of the solute with the micelles. Depending upon the nature of the solute and micelles the binding involves one or both of these interactions. The binding of a solute to

Table 3. Binding constants for ADDs with micelles.

Dye	Binding constant [$\times 10^{-3}$ M^{-1}]			
	SDS		CTAB	
	steady-state	time-resolved	steady-state	time-resolved
ADD **1**	18.2 ± 0.1	17.7 ± 0.3	4.1 ± 0.2	4.5 ± 0.1
ADD **2**	86.8 ± 2	90.3 ± 0.2	22.6 ± 0.5	23.2 ± 0.2

an ionic micelle is electrostatic when the strength of the interaction is determined by the charge density of the solute. In contrast, the binding of the solute with the micelles is hydrophobic when the strength of the binding is determined by the tendency of the solute to reduce its interaction with aqueous dipole. The binding of inorganic ions such as Ag^+, Cu^+, and Ni^+ with SDS micelles[28,29] is purely electrostatic and does not involve any covalent interactions with the sulfate groups on the micellar surface. The binding constants of aromatic hydrocarbons like benzene, anthracene, and pyrene are in the range 4×10^5–2×10^6 M^{-1} and correlate with the hydrophobicity of the solutes.[29]

ADD molecules are neutral and electrostatic interactions in the binding of ADDs with micelles are ruled out. The binding of these dyes is mainly attributed to hydrophobic interactions of the ADDs with the micelles. ADD **2** has a higher binding constant than ADD **1** in both types of micelle (SDS and CTAB). The additional methyl groups present at positions 3 and 6 of ADD **2** make it more hydrophobic and it binds strongly with micelles. From the fluorescence studies, it can be determined that the polarity of the ADD binding site in SDS is less than that in CTAB, that is, the ADD is solubilized in a more hydrophobic environment in SDS than in CTAB.

Laser flash photolysis of ADDs: The transient absorption spectrum of the ADDs in water with laser excitation at 355 nm shows maxima in the regions around 470 and 650 nm. The transient absorption spectra of ADD **1** in water is shown in Figure 3c. The transient decay observed above 600 nm has a short-lived component and a long-lived component. The short-lived decay is quenched by N_2O while the long-lived decay is unaffected by N_2O. Oxygen quenches the long-lived decay observed at 650 nm, while the 470 nm transient is not affected by oxygen. It is known that O_2 quenches the triplet state of the molecule and N_2O reacts with the solvated electron. The above observations lead to the conclusion that the 650 nm transient is due to triplet–triplet absorption[30] of ADD and the short-lived component observed above 600 nm (Figure 3b) is due to a hydrated electron. The hydrated electron reacts with the ADD and an anion radical is formed. The 470 nm transient absorption is assigned as anion-radical absorption which is in agreement with the findings of Mohan et al.[31]

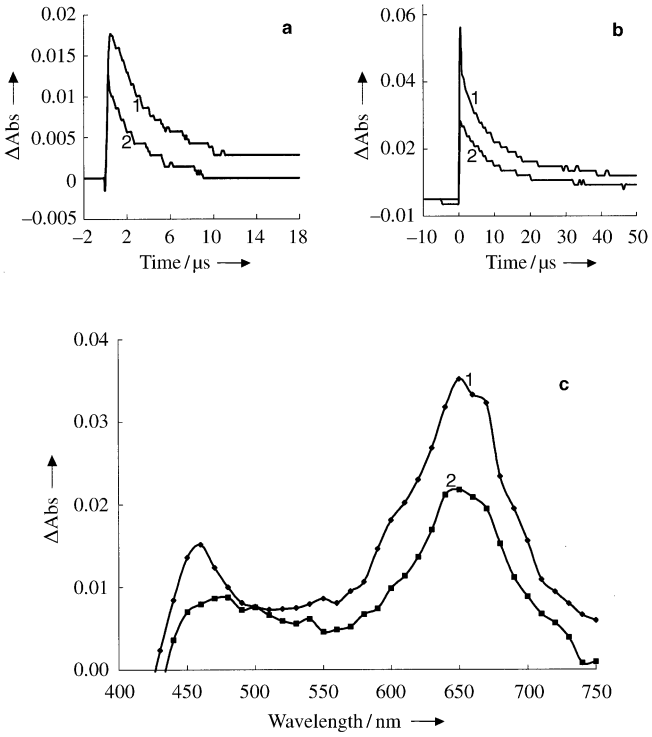

Figure 3. Transient decay monitored at a) 470 and b) 650 nm. c) Transient absorption spectrum of ADD **1** in water, recorded after 1 μs. In each case, trace 1 was measured with argon saturation and trace 2 was measured with N_2O saturation.

The transient absorption spectrum obtained from 355 nm laser flash photolysis of ADD **1** in 0.1 M SDS also shows transient maxima in the 470 and 650 nm regions (Figure 4d). These maxima are similar to those observed in water and are assigned to anion-radical and triplet–triplet absorption, respectively. In SDS, the transient decay observed above 600 nm also exhibits two decay components, similar to those observed in water. The absorption of the short-lived decay component is more intense in SDS than in water. The short-lived decay disappears in the presence of N_2O and is assigned to a hydrated electron, which is expected to have absorption in the region of 500–750 nm.[32] The decay of the hydrated electron at 720 nm is shown in Figure 4c.

In the presence of anionic micelles, the solvated electron absorbance and lifetime increase with an increase in the SDS concentration. In SDS, the electron exits from the micelles into the aqueous phase due to the electrostatic repulsion but the cation radical is strongly bound with the micelles due to the electrostatic attraction. The inhibition of the back reaction caused by the electrostatic barrier at the micelle–water interface enhances the yield and lifetime of the solvated electron. One route of decay of the electron is through reaction with the ground state of the ADD molecule. The observation of the anion-radical transient at 470 nm in SDS indicates the occurrence of the reaction of a hydrated electron with the ADD. The rate of decay and absorbance of the hydrated electron increases with increase in the concentration of ADD molecules and is represented in Figure 5. The decay of the hydrated electron is analyzed by

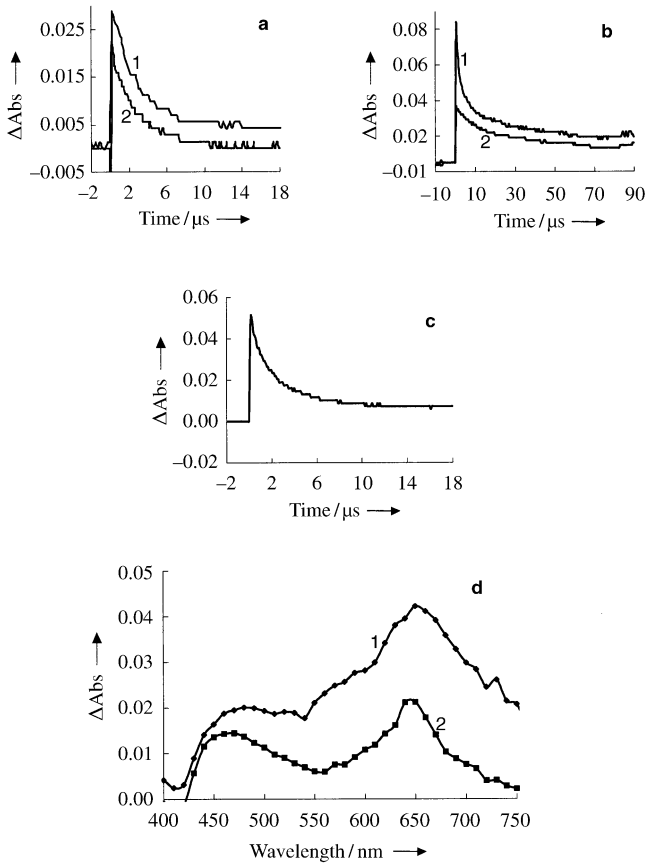

Figure 4. Transient decay monitored at a) 470, b) 650, and c) 720 nm. d) Transient absorption spectrum of ADD **1** in 0.1 M SDS, recorded after 1 μs. In each case, trace 1 was measured with argon saturation and trace 2 was measured with N_2O saturation.

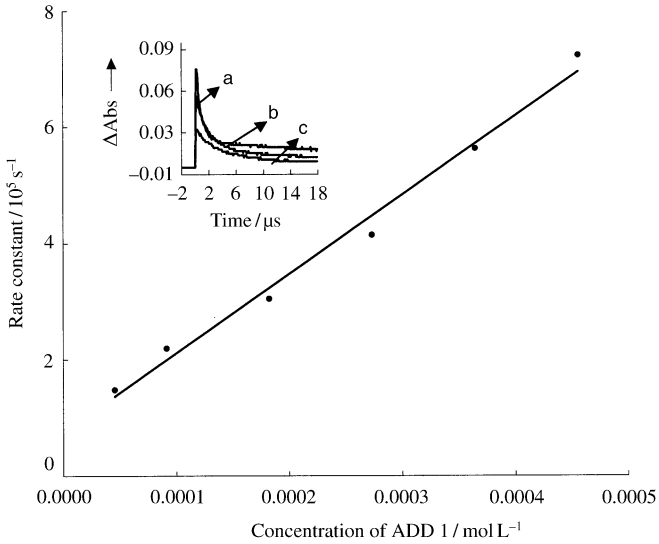

Figure 5. Plot of pseudo-first-order rate constant of hydrated electron decay at 720 nm against concentration of ADD **1**. Inset: Decay of the hydrated electron with a) 4.5×10^{-5}, b) 9×10^{-5}, and c) 3.6×10^{-4} M ADD **1**.

pseudo-first-order kinetics and from the plot; the bimolecular rate constant for the reaction of ADD with the electron is calculated to be $1.4\pm0.5\times10^{9}\,M^{-1}s^{-1}$. The rate constant obtained in homogeneous solution[31] ($2–5\times10^{10}\,M^{-1}s^{-1}$) is higher than the value observed in SDS. In the presence of anionic micelles, the ejected electron is repelled by the negatively charged surface of the micelles containing the neutral ADD molecules. In micelles, the ADDs are partitioned between the aqueous and micellar phases and hence the hydrated electron reacts only with ADD molecules that are present in the aqueous phase. If ADDs exist as dimers in the Stern layer, then the electron formed would react within the Stern layer. But we observe an enhancement in the yield and lifetime of the solvated electron with increasing SDS concentration. This clearly indicates that the solvated electron reacts with ADD molecules present in the aqueous phase only, a result that further supports the absence of dimers in the Stern layer.

The transient absorption spectra of the ADDs in CTAB show much more similarity to the absorption curves obtained in aqueous solution than to those observed in SDS. In CTAB, the triplet–triplet absorption of the ADD increases with increase in the concentration of CTAB whereas no such behavior is observed in the case of SDS. The triplet–triplet absorption spectrum of ADD **1** in solutions with different concentrations of CTAB are shown in Figure 6. The

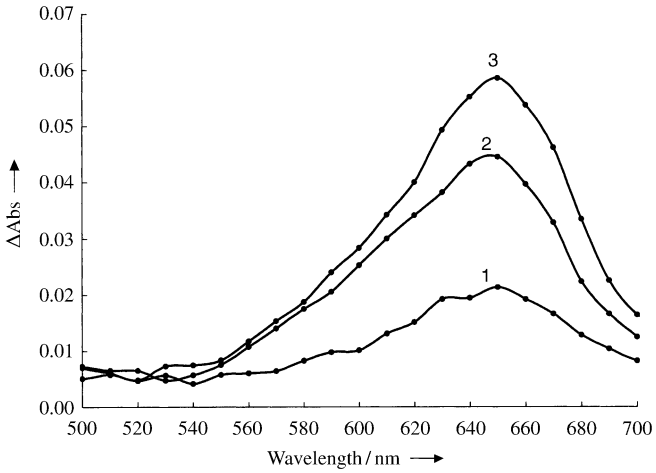

Figure 6. Triplet–triplet absorption spectrum of ADD **1** in water with CTAB concentrations of a) 0.04, b) 0.07, and c) 0.1 M, recorded 2 μs after the laser pulse.

charge on the micelles plays a crucial role in the efficiency of the separation of the products of the photoionization process. The electron is not able to escape easily from the cationic micelle because of the electrostatic attraction, the recombination of the cation radical and the electron is more efficient, and the yield of hydrated electron is lower in the cationic micelle. The recombination reaction favors the triplet induction when the ion-pair energy is higher than the triplet state of the ADD. The enhanced triplet absorption in cationic micelles (CTAB) is nicely explained by the triplet induction by the ion-pair recombination.

Cation radicals of ADDs: The transient decay of ADD molecules monitored at 440 nm shows residual absorbance and

is much stronger in solutions of SDS and CTAB than in pure water. The transient absorption of ADD **1** in 0.1 M SDS recorded 15 μs after the laser pulse shows a maximum at 440 nm (Figure 7), which is assigned to the cation radical of

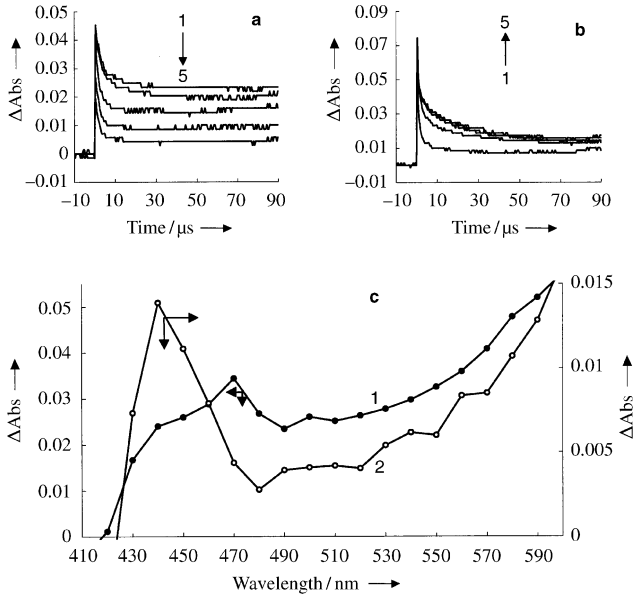

Figure 7. The effect of pH value on the transient decay of ADD **1** in 0.1 M SDS, monitored at a) 440 and b) 550 nm. In each case, the pH values were as follows: 1) 7, 2) 5, 3) 4, 4) 3.5, and 5) 3.0. c) The transient absorption spectrum of ADD **1** in 0.1 M SDS at pH 7, 1) 1 and 2) 15 μs after the pulse.

the ADD. In a pulse radiolysis study Mohan and Mittal[33] reported that the cation radical has absorption at 440 nm and a broad band at 600–700 nm. The assignment of the 440 nm transient to the cation radical is therefore in agreement with the pulse radiolysis studies.

Acridinedione dyes have structural similarity to NADH and the cation radicals of NADH model compounds have been studied extensively.[34] The radical cations generated from NADH model compounds undergo keto–enol tautomerization proceeded by a [1,4] hydrogen shift. Recently Fuzukumi et al.[35] reported the tautomerization of radical cations of NADH analogues by using ESR and flash photolysis techniques. They generated the radical cation of 1-benzyl-1,4-dihydronicotinamide (BNAH) through thermal and photoinduced electron transfer reactions in acetonitrile. The keto and enol radical cations of BNAH show absorption maxima at 400 and 460 nm, respectively.

On decreasing the pH value, the residual absorbance at 440 nm decreases, with a simultaneous increase at 550 nm. The effect of the pH value on the 440 and 550 nm transients in SDS is shown in Figures 7a and b,respectively. Marcinek et al.[36] reported that under acidic conditions an enol radical cation of ADD is formed that has absorption at 550 nm. The 440 nm transient is assigned to the keto form of the ADD cation radical. The transient maximum of the ADD radical cations in aqueous micellar solutions is significantly red shifted relative to the maximum of the radical cations of BNAH in acetonitrile.[35] Above pH 5 the ADD cation radical exists in the keto form and below pH 4 it exists in the enol form. In the intermediate pH range both the keto and enol forms of the radical cation coexist under equilibrium. The pK_a value of the enol radical cation was determined to be around 4.5 in SDS and around 3.0 in CTAB. In acidic conditions, the formation of the enol radical cation is facilitated by the protonation at the carbonyl oxygen atom and is similar to the acid-catalyzed keto–enol tautomerization of α,β-unsaturated carbonyl compounds. The transient absorption spectra of ADDs recorded in water, SDS, and CTAB under acidic conditions (pH 3.5) show transient absorption maxima at 590 nm (see Figure 8 for the spectrum in SDS).

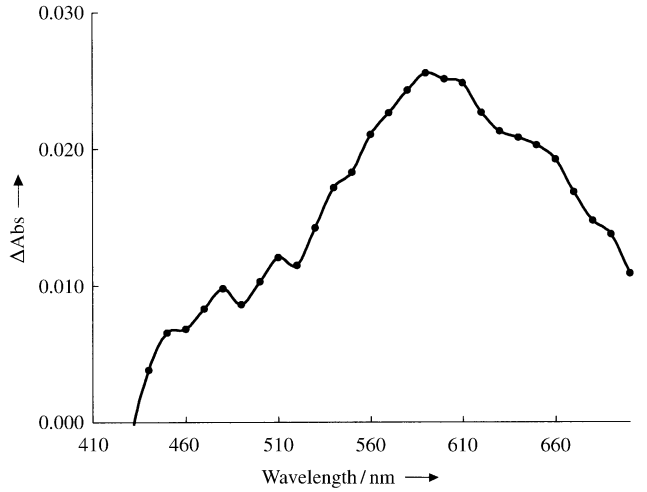

Figure 8. Transient absorption spectrum of ADD **1** in 0.1 M SDS at pH 4.5.

In the pulse radiolysis reduction of the ADD^+ molecule, Marcinek et.al.[34] reported that the carbon-centered radical and enol cation radical are in equilibrium and under such circumstances they have a transient absorption maximum at 590 nm. A similar observation in the present investigation suggests that in the pH range below 4, the enol cation radical and the carbon-centered radical are in rapid equilibrium. In the present study we find that the enol radical cation of acridinedione dyes is formed from the keto form of the cation radical and, depending on the pH value of the medium, either the keto or enol form of the cation radical will exist. The photooxidation and the subsequent reactions of the ADDs are represented in Scheme 1.

Comparison of the oxidation of NADH with ADD oxidation: The mechanism of NADH oxidation was established by use of model compounds (1,4-dihydropyridine derivatives) and several mechanisms, such as one-step hydride transfer and multistep electron–proton transfer, have been proposed for the oxidation of NADH to NAD^+. The detection of the radical cation in thermal, electrochemical, and photochemical oxidations of NADH has confirmed the sequential electron–proton–electron transfer mechanism. Deprotonation of the cation radical leads to the carbon-centered radical, which undergoes a further one-electron oxida-

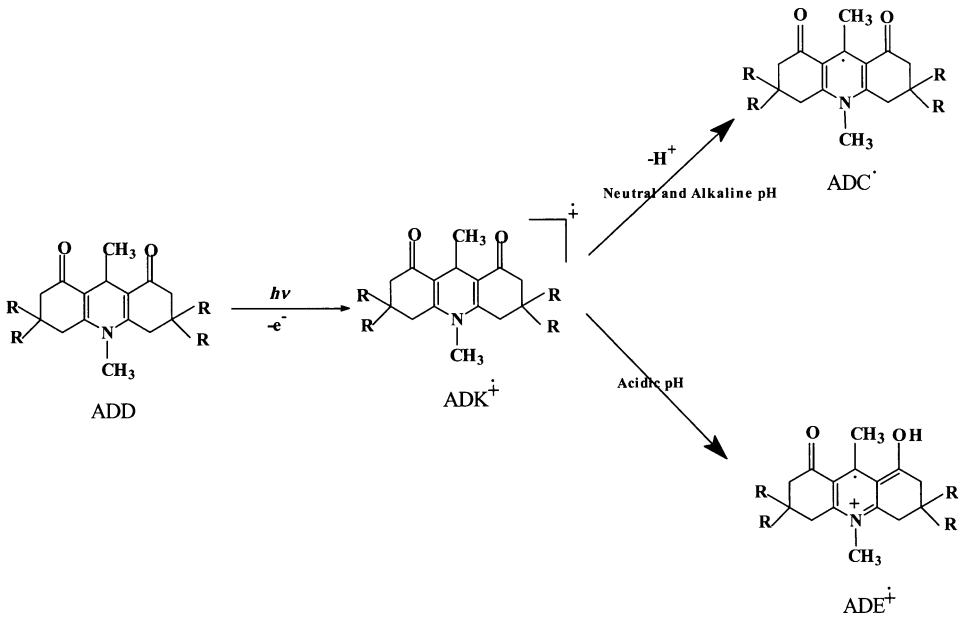

Scheme 1. Mechanism of acridinedione dye oxidation. ADD = acridinedione dye, $ADK^{\cdot+}$ = keto radical cation, ADC· = carbon-centered radical, $ADE^{\cdot+}$ = enol radical cation.

tion to give NAD^+. Marcinek et al. reported the formation of tautomeric enol radical cations from the oxidation of NADH model compounds.[34] The enol radical cation formed by the deprotonation–reprotonation processes from the keto radical cation. They also studied the reverse stepwise transformation of NAD^+ to NADH; this process occurs by protonation of the carbon-centered radical at the oxygen atom resulting in the enol radical cation. The enol form of cation radical reverts rapidly to the more stable keto form on neutralization. The mechanism proposed by Marcinek et al.[34] illustrates the sequential electron–proton–electron transfer in the NADH⇄NAD^+ transformation and includes the two tautomeric forms of the NADH radical cation but the authors do not indicate the effect of the pH value on the formation of the cation radicals. From the photooxidation of ADDs in micelles (Scheme 1), we have concluded that the mechanistic pathway of oxidation (thermal and photochemical) of NADH to NAD^+ depends on the pH value of the medium (Scheme 2). In alkaline conditions, the deprotonation of the keto cation radical ($NADHK^{\cdot+}$) results in the carbon-centered radical (NAD·), which further undergoes one-electron oxidation to give NAD^+. In acidic conditions, the keto form of the cation radical is converted into the enol radical cation ($NADHE^{\cdot+}$) through a [1,4] hydrogen shift. The enol radical cation is in equilibrium with the carbon-centered radical, which can undergo further oxidation as above (Scheme 2). From this study we also conclude that the reverse reaction, that is, conversion of NAD^+ into NADH, is possible only in acidic conditions.

Monophotonic and biphotonic ionization: The photonicity of photoionization processes in aqueous homogeneous solutions could not be evaluated due to the poor yield of solvated electrons. In SDS, the yield of solvated electrons is quite large and this helps to identify the mechanism of photoionization of the ADDs. The absorbance of the solvated electrons is measured as a function of the laser intensity. The ADD solubilized in SDS micellar solutions was excited by 248 and 355 nm laser pulses of different intensities and the absorbance of the solvated electrons at 720 nm was monitored after a 200-ns delay. The absorbance of the solvated electrons can be described as a function of the laser intensity as given by Equation (13), where OD is the optical density of the solvated electrons at 720 nm, E_t is the pulse energy, n is an integer, and k is a constant encompassing the specified experimental conditions. The value of n can be determined from the double log plot of Equation (13) as described by Equation (14).

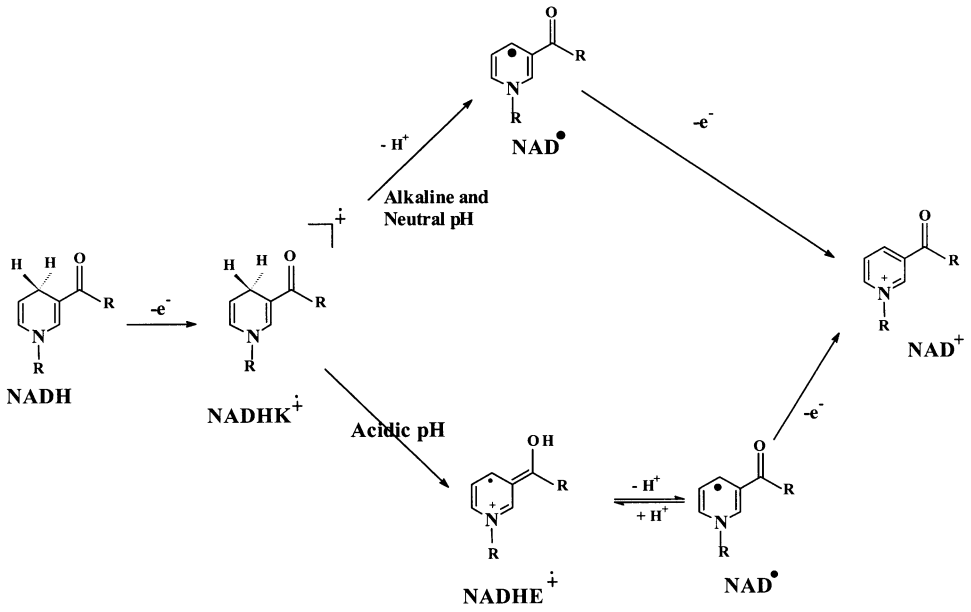

Scheme 2. Mechanism of NADH oxidation based on acridinedione dye oxidation in micelles.

$$OD = kE_t^n \quad (13)$$

$$\log(OD) = \log(k) + n\log(E_t) \quad (14)$$

Figure 9 presents the plot of log(OD) against log(E_t) for ADD **1** in SDS micellar solution. For experiments with excitation at 355 nm the slope is determined to be 2.08 and excitation with 248 nm yields a slope of 1.1. Hence, it can be concluded that the photoionization of ADDs by 248 nm light proceeds by a monophotonic ionization process, while that at 355 nm occurs through a biphotonic process.

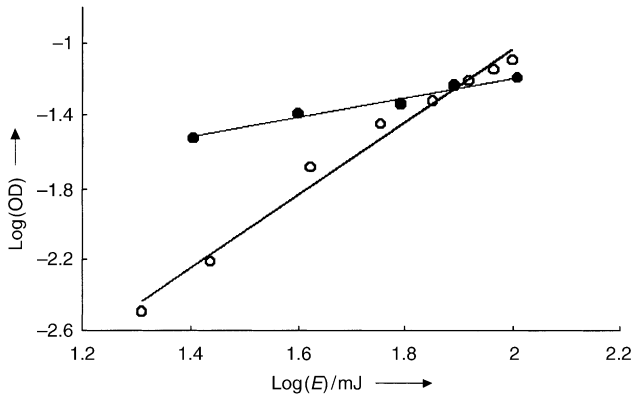

Figure 9. Plot of log(OD) against log(E_t) for electron yields from ADD **1** in 0.1 M SDS.

There are several reports on photoionization of solutes in micellar media. Aromatic hydrocarbons such as pyrene, perylene, and tetracene photoionize[18] by a biphotonic process, whereas aromatic amines with low oxidation potentials such as tetramethylbenzidine[37] and phenothiazine[38] undergo monophotonic ionization. Photoionization of phenothiazine has been studied extensively in homogeneous and micellar solutions and it has been reported that the photoionization process depends on the excitation wavelength.[39] In aqueous SDS micellar solutions, the photoionization of phenothiazine is found to be monophotonic at 266 nm, but both mono- and biphotonic processes seem to operate at 355 nm. It was concluded that the photoionization occurs from the higher excited singlet state of phenothiazine.

The wavelength-dependent photonicity of the acridinedione dyes in SDS micellar solutions exemplifies the involvement of higher excited states in the photoionization. Excitation with 248 nm photons directly promotes electrons from the S_0 to S_2 state and the photoionization proceeds by a monophotonic process. Excitation at 355 nm promotes the electrons to the S_1 state by the absorption of one photon and subsequent absorption of one more photon promotes the electrons to the S_2 state (Scheme 3).

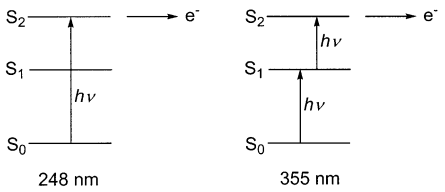

Scheme 3. Monophotonic and biphotonic ionization of ADD dyes.

Conclusion

The absorption and fluorescence spectral characteristics of the ADDs in SDS and CTAB reveal that they are solubilized in a less polar environment than water. The polarity of the binding site of the dyes in the micelles was determined and the probe is solubilized in the Stern layer, that is, at the micelle–water interface, with the dye more exposed to water. In the micellar environment the fluorescence intensity of the ADDs is enhanced. The biexponential nature of fluorescence decay of the ADDs in micelles confirms that the dyes are in two different environments, that is, they are in equilibrium between the aqueous and micellar phases. The binding constants of the ADDs with the SDS and CTAB micelles were determined and indicate a hydrophobic interaction between the micelles and the ADDs. Formation of solvated electrons is observed for acridinedione dyes with laser flash photolysis for the first time. It has been observed that ionization is monophotonic upon excitation at 248 nm and a stepwise biphotonic process occurs at 355 nm. In cationic micelles, the recombination of the cation radical and the electron results in the formation of the triplet state. Cation radicals derived from the photooxidation of ADD molecules are involved in keto–enol tautomerization. The enol radical cations of acridinedione dyes are formed from the keto form of the cation radicals by intramolecular hydrogen transfer. The results of the present study were compared with the existing mechanisms for photooxidation of NADH and by using this study we have pointed out that the intermediate cation radical involved in the oxidation of NADH depends on the pH value of the biological system.

Experimental Section

ADDs have been synthesized by the procedure reported in the literature.[10,40] SDS (Sisco Research Laboratory) and CTAB (Fluka Chemicals) were checked to be fluorescence free and then used as received. Triply distilled water was used for solution preparation. All other solvents used were HPLC grade as obtained from Qualigens, India. The absorption spectra were recorded by using a Hewlett–Packard 8542A diode-array spectrophotometer. The fluorescence experiments were carried out by using a Perkin–Elmer LS5B spectrofluorimeter. The concentration of ADDs used was 1×10^{-5} M. The stock solutions of ADDs were prepared in water/methanol (99.5:0.5 v/v). The emission spectra were recorded by exciting the sample at the isosbestic wavelength.

Laser flash photolysis was performed by using the third harmonic of an Nd:YAG laser ($\lambda = 355$ nm, DCR-2, Spectra Physics) and a KrF excimer laser ($\lambda = 248$ nm, Lexrta-50, Lambda Physik). The transient absorption changes were monitored perpendicular to the laser beam by using a 300 W pulsed Xenon arc lamp. The transient signals were detected with a Hamamatsu R-928 photomultiplier. The photomultiplier output was digitized with a 100-MHz digital storage oscilloscope (Hewlett–Packard 54201A) interfaced to a computer. Kinetic analyses were carried out by using the software described elsewhere.[41] For all studies the solutions were deaerated by purging with argon gas for 30 min prior to the experiments.

Time-resolved fluorescence decays were obtained by the time-correlated single-photon-counting (TCSPC) method. A diode-pumped Milliena V CW laser (Spectra Physics, 532 nm) was used to pump the Ti-Sapphire rod in a Tsunami picosecond-mode locked laser system (Spectra Physics). The 750 nm (85 MHz) beam from the Ti-Sapphire laser was passed through a pulse picker (Spectra Physics, 3980 2S) to generate 4 MHz pulses. The second harmonic output (375 nm) was generated by a flexible harmonic generator (Spectra Physics, GWU 23PS). A vertically polarized 375 nm laser was used to excite the sample. The fluorescence emission at the magic angle (54.7°) was counted by an MCP PMT apparatus (Hamamatsu R3809U) after being passed through the monochromator and was processed through a constant fraction discriminator (CFD), a time-to-amplitude converter (TAC) and a multichannel analyzer (MC). The instrument response function for this system is $\approx$52 ps. The fluorescence decay was obtained and was further analyzed by using IBH (UK) software (DAS-6).

Acknowledgement

Financial support from the Department of Science and Technology, Government of India, through the National Centre for Ultrafast Processes is much appreciated. A Fellowship received by C.S. from CSIR is gratefully acknowledged.

[1] a) R. C. Bohinski, *Modern Concepts in Biochemistry*, 3rd ed., Allyn & Bacon, Boston, **1997**; b) L. Stryer, *Biochemistry*, 4th ed., Freeman, New York, **1995**.
[2] a) B. N. Carlson, L. L. Miller, *J. Am. Chem. Soc.* **1985**, *107*, 479–485; b) S. Fukusumi, S. Koumitsu, K. Hirinaka, T. Tanaka, *J. Am. Chem. Soc.* **1987**, *109*, 305–316; c) M. M. Kreevoy, D. Ostovic, I. S. Lee, D. A. Blinder, G. W. King, *J. Am. Chem. Soc.* **1988**, *110*, 524–530; d) L. L. Miller, J. R. Valentine, *J. Am. Chem. Soc.* **1988**, *110*, 3982–3989.
[3] a) S. Fukuzumi, N. Nishizawa, T. Tanaka, *J. Org. Chem.* **1984**, *49*, 3571–3578; b) S. Inagaki, Y. Hirabayashi, *Bull. Chem. Soc. Jpn.* **1977**, *50*, 3360–3364; c) C. Pac, M. Ihama, M. Yasuda, Y. Miyauchi, H. Sakurai, *J. Am. Chem. Soc.* **1981**, *103*, 6495–6497.
[4] a) A. Anne, P. Hapiot, J. Moiroux, P. Neta, J. M. Saveant, *J. Am. Chem. Soc.* **1992**, *114*, 4694–4701; b) P. Hapiot, J. Moiroux, J. M. Saveant, *J. Am. Chem. Soc.* **1990**, *112*, 1337–1343.
[5] a) S. Fukuzumi, T. Suenobu, T. Patz, S. Itoh, M. Fujitsuka, O. Ito, *J. Am. Chem. Soc.* **1998**, *120*, 8060–8068; b) A. Anne, J. Moiroux, J. M. Saveant, *J. Am. Chem. Soc.* **1993**, *115*, 10224–10230; c) J. P. Cheng, Y. Lu, X. Zhu, L. Mu, *J. Org. Chem.* **1998**, *63*, 6108–6114; d) X.-Q. Zhu, H.-R. Li, Q. Li, T. Ai, J.-Y. Lu, Y. Yang, J.-P. Cheng, *Chem. Eur. J.* **2003**, *9*, 871–880.
[6] a) S. Fukuzumki, T. Tanaka in *Photoinduced Electron Transfer* (Eds.: M. A. Fox, M. Chanon), Elsevier, Amsterdam, **1998**, part C, pp. 578–635; b) U. Bruehlmann, E. Hayon, *J. Am. Chem. Soc.* **1974**, *96*, 6169–6175; c) D. J. Creighton, J. Hajdu D. S. Sigman, *J. Am. Chem. Soc.* **1976**, *98*, 4619–4625; d) S. Fukuzumi, S. Mochizuki, T. Tanaka, *J. Chem. Soc. Dalton Trans.* **1990**, 695–697.
[7] a) K. J. Prabahar, V. T. Ramakrishnan, D. Sastikumar, S. Selladurai, V. Masilamani, *Indian J. Pure Appl. Phys.* **1991**, *29*, 382–384; b) P. Murugan, P. Shanmugasundram, V. T. Ramakrishnan, B. Venkatachalapathy, N. Srividya, P. Ramamurthy, K. Gunasekaran, D. Velmurugan, *J. Chem. Soc. Perkin Trans. 2* **1998**, 999–1003.
[8] S. Singh, S. Chhina, V. K. Sharma, S. S. Sachdev, *J. Chem. Soc. Chem. Commun.* **1982**, 453–454.
[9] a) A. Fleckenstein, *Annu. Rev. Pharmacol. Sci.* **1987**, *17*, 149–166; b) R. A. Jains, P. Silver, D. J. Triggle, *Adv. Drug Res.* **1987**, 16, 309–315; c) B. Love, M. M. Goodman, K. M. Snader, R. Jadeschi, E. Macko, *J. Med. Chem.* **1974**, *17*, 956–965.
[10] N. Srividya, P. Ramamurthy, P. Shanmugasundram, V. T. Ramakrishnan, *J. Org. Chem.* **1996**, *61*, 5083–5089.
[11] a) N. Srividya, P. Ramamurthy, V. T. Ramakrishnan, *Spectrochim. Acta* **1998**, *54*, 245–253; b) N. Srividya, P. Ramamurthy, V. T. Ramakrishnan, *Spectrochim. Acta* **1997**, *53*, 1743–1753.
[12] a) B. Venkatachalapathy, P. Ramamurthy, *Phys. Chem. Chem. Phys.* **1999**, *1*, 2223–2230; b) C. Selvaraju, A. Sivakumar, P. Ramamurthy, *J. Photochem. Photobiol. A* **2001**, 138, 213–226.
[13] H. T. Q. Witt, *Q. Rev. Biophys.* **1971**, *4*, 365–377.
[14] B. Czochralska, L. Lindqvist, *Chem. Phys. Lett.* **1983**, *101*, 297–299.
[15] a) L. Lindqvist, B. Czochralska, I. Grigorov, *Chem. Phys. Lett.* **1985**, *119*, 494–498; b) D. W. Boldridge, T. H. Morton, G. W. Scott, *Chem. Phys. Lett.* **1984**, *108*, 461–465.
[16] a) J. H. Fendler, *Membrane Mimetic Chemistry*, Wiley Interscience, New York, **1982**; b) K. Kalyansundaram, *Photochemistry in Microheterogeneous Systems*, Academic Press, Orlando, **1987**.
[17] N. J. Turro, M. Gratzel, B. M. Braun, *Angew. Chem.* ***1980,*** *92*, 712–734; *Angew. Chem. Int. Ed. Engl.* **1980**, *19*, 675–696.
[18] a) T. Iwaoka, M. Kondo, *Chem. Lett.* **1978**, 731–735; b) R. Humphry-Baker, A. M. Braun, M. Gratzel, *Helv. Chim. Acta* **1981**, *64*, 2036–2047; c) S. A. Alkaities, G. Beck, M. Gratzel, *J. Am. Chem. Soc.* **1975**, *97*, 5723–5729; d) S. C. Wallace, M. Gratzel, J. K. Thomas, *Chem. Phys. Lett.* **1973**, *23*, 359–362.
[19] a) J. K. Thomas, P. Piciulo, *J. Am. Chem. Soc.* **1978**, *100*, 3239–3240; b) J. K. Thomas, P. Piciulo, *J. Am. Chem. Soc.* **1979**, *101*, 2502–2503.
[20] a) K. Kalayanasundaram, J. K. Thomas, *J. Am. Chem. Soc.* **1977**, *99*, 2039–2044; b) P. Mukerjee, K. J. Mysels in *Critical Micelle Concentration of Aqueous Surfactant Systems, Vol. 36*, NSRDS-NBS, Washington DC, **1971**.
[21] a) R. S. Sarpal, M. Belletete, G. Durocher, *J. Phys. Chem.* **1993**, *97*, 5007–5013; b) R. Das, D. Guga, S. Mitra, S. Kar, S. Lahiri, S. Mukherjee, *J. Phys. Chem. A* **1997**, *101*, 4042–4047; c) A. G. Mwalupindi, A. Rideau, R. A. Agbaria, I. M. Warner, *Talanta* **1994**, *41*, 599–609.
[22] H. Chouchaing, A. Lukton, *J. Phys. Chem.* **1975**, *79*, 1935–1939.
[23] a) R. H. Baker, R. Steiger, M. Gratzel, *J. Am. Chem. Soc.* **1980**, *102*, 847–848; b) A. K. Ghosh, *Indian J. Chem.* **1974**, *12*, 313–314; c) R. C. Kapoor, V. N. Mishra, *J. Indian Chem. Soc.* **1976**, *53*, 965–967; d) P. Mukerjee, K. J. Mysels, *J. Am. Chem. Soc.* **1955**, *77*, 2937–2943.
[24] a) V. V. Bagdasarian, A. A. Shahinyan, *Colloid J.* **1977**, 59, 136–142; b) V. V. Bagdasarian, A. A Shahinyan, *Mol. Cryst. Liq. Cryst.* **1994**, *241*, 55–68.
[25] H. A. Benesi, J. H. Hildebrand, *J. Am. Chem. Soc.* **1949**, *71*, 2703–2707.
[26] L. E. Cramer, K. G. Spears, *J. Am. Chem. Soc.* **1978**, *100*, 221–227.
[27] C. Hirose, L. Sepulveda, *J. Phys. Chem.* **1981**, *85*, 3689–3694.
[28] J. B. S. Bonilha, T. K. Foreman, D. G. Whitten, *J. Am. Chem. Soc.* **1982**, *104*, 4215–4220.
[29] M. Fischer, P. D. I. Fletcher, W. Knoche, B. H. Robinson, N. C. White, *Colloid Polym. Sci.* **1980**, 258, 733–738.
[30] N. Srividya, P. Ramamurthy, V. T. Ramakrishnan, *Phys. Chem. Chem. Phys.* **2000**, *2*, 5120–5126.
[31] H. Mohan, J. P. Mittal, B. Venkatachalapathy, N. Srividya, P. Ramamurthy, *J. Chem. Soc. Faraday Trans.* **1997**, 93, 4269–4274.
[32] E. J. Hart, M. Anbar, *The Hydrated Electron*, Wiley Interscience, New York, **1970**.
[33] H. Mohan, J. P. Mittal, *J. Photochem. Photobiol. A* **2001**, 141, 25–32.
[34] a) A. Marcinek, J. Adamus, J. Rogowski, J. Gebicki, P. Bednarek, P. Bally, *J. Phys. Chem. A* **2000**, *104*, 718–723; b) A. Marcinek, J. Adamus, K. Huben, J. Gebicki, T. J. Bartczak, P. Bednarek, P. Bally, *J. Am. Chem. Soc.* **2000**, *122*, 437–443.
[35] a) S. Fuzukumi, O. Inada, T. Suenobu, *J. Am. Chem. Soc.* **2002**, 124, 14538–14539; b) S. Fuzukumi, O. Inada, T. Suenobu, *J. Am. Chem. Soc.* **2003**, *125*, 4809–4816.
[36] A. Marcinek, J. Adamus, J. Rogowski, J. Gebicki, T. J. Bartczak, P. Bednarek, P. Bally, *J. Phys. Chem. A* **2000**, *104*, 724–728.
[37] S. A. Alkaitis, M. Gratzel, *J. Am. Chem. Soc.* **1976**, *98*, 3549–3554.
[38] J. K. Thomas, P. Piciulo, *J. Am. Chem. Soc.* **1978**, *100*, 3239–3240.
[39] H. N. Ghosh, A. V. Sapre, D. K. Palit, J. P. Mittal, *J. Phys. Chem. B* **1997**, *101*, 2315–2320.
[40] P. Shanmugasundaram, P. Murugan, V. T. Ramakrishnan, N. Srividya, P. Ramamurthy, *Heteroatom Chem.* **1996**, *7*, 17–22.
[41] P. Ramamurthy, *Chem. Educ.* **1993**, *9*, 56–60.

Received: November 3, 2003 [F5678]